Oceanographic Expert System Validation Using GOAP Mesoscale Products and Gulfcast/DART Validation Test Data

AD-A226 929

DTIC
ELECTE
SEP 27. 1990
B

M. Lybanon
Remote Sensing Branch
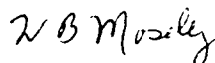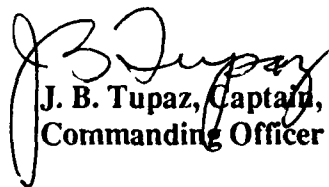**Ocean Sensing and Prediction Division**
Ocean Science Directorate

Foreword

Present interpretive methods applied to satellite ocean imagery interpretation are largely manual, require significant effort, and are highly dependent on the interpreter's skill. During the early 1990s the U.S. Navy will face an unprecedented wealth of new remotely sensed data available from U.S. (e.g., Spinsat, TOPEX/Poseidon) and foreign (European ERS-1, Japanese ERS-1) satellites, and some present-day satellites will continue to supply oceanographic data as well. The sheer volume of data from these satellites will be overwhelming to analysts, and anticipated manpower reductions will dictate a need for greater automation.

The Naval Oceanographic and Atmospheric Research Laboratory has developed a prototype expert system, whose rule base is derived from an unprecedented compilation of information about mesoscale features in the Gulf Stream region, and whose mode of operation is innovative. This report presents validation test results that show the expert system provides useful hypotheses about ring motion and size variation for periods up to several weeks. Since an operation interpreter may be required to provide analyses at regular intervals, even during data-sparse periods, this expert system has the potential to be a valuable component of a completely automated interpretation system for oceanographic imagery.

W. B. Moseley
Technical Director

J. B. Tupaz, Captain, USN
Commanding Officer

Executive Summary

A prototype oceanographic expert system is being developed by the Remote Sensing Branch of the Naval Oceanographic and Atmospheric Research Laboratory (NOARL). System performance for eddy motion was tested using GEOSAT Ocean Applications Program (GOAP) mesoscale products. A second data set was used to validate the Harvard Gulfcast and the NOARL DART (Data Assimilation Research and Transition program) models.

Several types of performance measures were calculated for both warm- and cold-core Gulf Stream eddies. Statistics compiled from the analysis results are presented in both tabular and graphical form. The analysis shows that the expert system performs reasonably well with respect to both eddy motion and eddy size. The expert system's projections are superior to an assumption of no motion out to 14 days. Results with the second (better) data set indicate performance superior to no motion in about two-thirds of the cases. The GOAP results, which used longer sequences, indicate that the cold-core ring rules perform well for periods longer than 2 weeks. The expert system tracks ring sizes to within 10% for periods up to 7-11 weeks.

Discussion of the results identifies factors that interfere with the validation and strongly indicates the need for more data to continue and refine the analysis. A first-order correction to the rule base is proposed, based on the results of this study. That correction should significantly improve the expert system's average eddy motion performance. Changes based upon a more detailed evaluation may also be feasible and could lead to greater improvements.

i

Acknowledgments

Contents

Oceanographic Expert System Validation Using GOAP Mesoscale Products and Gulfcast/DART Validation Test Data

1. Introduction

Satellite imagery of the oceans has become an invaluable tool for the oceanographer. These imagery add the breadth of synoptic coverage to the depth of in situ measurements at a few points. The deluge of satellite data that soon will be easily available to the U.S. Navy, as well as the labor-intensive nature of current interpretive methods, will pose severe problems for operational interpreters. The Remote Sensing Branch of the Naval Oceanographic and Atmospheric Research Laboratory is developing knowledge-based techniques to remove some of this burden from the interpreter.

One tool under development is an expert system with a knowledge (rule) base containing information about mesoscale oceanographic features in the Gulf Stream region of the North Atlantic Ocean (Lybanon et al., 1986; Thomason and Blake, 1986; Thomason, 1987). The prototype expert system's domain is a sequence of registered satellite infrared images. The events represented in the knowledge base are landmass boundaries, warm-core rings (WCR), cold-core rings (CCR), the Gulf Stream's north and south walls, and areas on the Gulf Stream boundaries in which rapid changes are occurring in local regions. The expert system's rule base concentrates on the time evolution of the features. As such, it could be valuable to an interpreter who must "fill in" information when adverse conditions, such as extensive cloud cover or missed "passes," prevent the addition of new observations since a previous analysis. It must be emphasized that this system was not designed as a "stand-alone" simulation to give accurate, long-term predictions; rather, the system should be regarded as forming hypotheses about the evolution of mesoscale features which must then be validated as much as possible by evidence from satellite and in situ data.

The expert system must be validated to quantify the confidence an analyst can have in its results. The ring motion and size variation rules are more highly developed than the Gulf Stream motion logic, so that portion was chosen for validation first. This report describes the testing and analysis procedure that was used in the first

comprehensive validation and presents the results. The rule base was the most current in an evolving sequence of implementations. Details of the version tested are presented in Appendix A.

2. Expert System Validation Procedure Outline

Validation of any software involves the difficult task of insuring that it meets carefully designed criteria of adequacy. In the case of an expert system rule base for mesoscale dynamics in the Gulf Stream region, the ideal criterion is faithfulness to real ocean dynamics. However, ocean "truth" is not easily obtained. What one must settle for is a mesoscale analysis produced by human interpretation of observed data. Since the analysis is a human interpretation of sketchy data rather than direct observation, that analysis will contain errors. However, for the sake of this validation study the human analysis is assumed to be truth. The scheme for development of the knowledge base is, then, development of the first-generation rule set, testing against ocean truth, and refinements to produce an improved second-generation rule set.

The expert system to be tested here starts with the "state" (i.e., locations, sizes, and identities of mesoscale features) of the Gulf Stream region at one time and generates hypotheses about the states at consecutively later times. Performance testing, then, requires comparison of these hypotheses with mesoscale analyses of the same region for the later times.

We chose two data sets both to determine the initial state of the expert system and to compare with the expert system output. The first set consisted of GEOSAT Ocean Applications Program (GOAP) mesoscale products. The GOAP products list (1) the positions of points along the Gulf Stream's north and south walls and (2) the center coordinates and sizes of WCRs and CCRs. They were produced by an expert oceanographer and include information from GEOSAT altimeter data, satellite imagery, and bathythermograph data

(Lybanon and Crout, 1987). Figures 1 and 2 outline the test plan followed. Each member of a sequence of GOAP products was used to initialize the expert system, which subsequently calculates the positions and sizes of WCRs and CCRs 7, 14, . . . days later (the 7-day interval could be changed). For each set of outputs, the estimate for N days after the initial state (N = 7, 14, . . .) was compared with the GOAP product of the equivalent date.

We used three sequences of GOAP products at 7-day intervals for testing (Table 1). Tracey and Watts (1986) presented statistics that show that the along-stream average Gulf Stream position between 50° and 75°W is farthest south in April and farthest north in November. So, we chose sequences centered about those months to ensure that the expert system would be tested for a variety of conditions. We also chose periods for which high-quality satellite imagery were available so that we
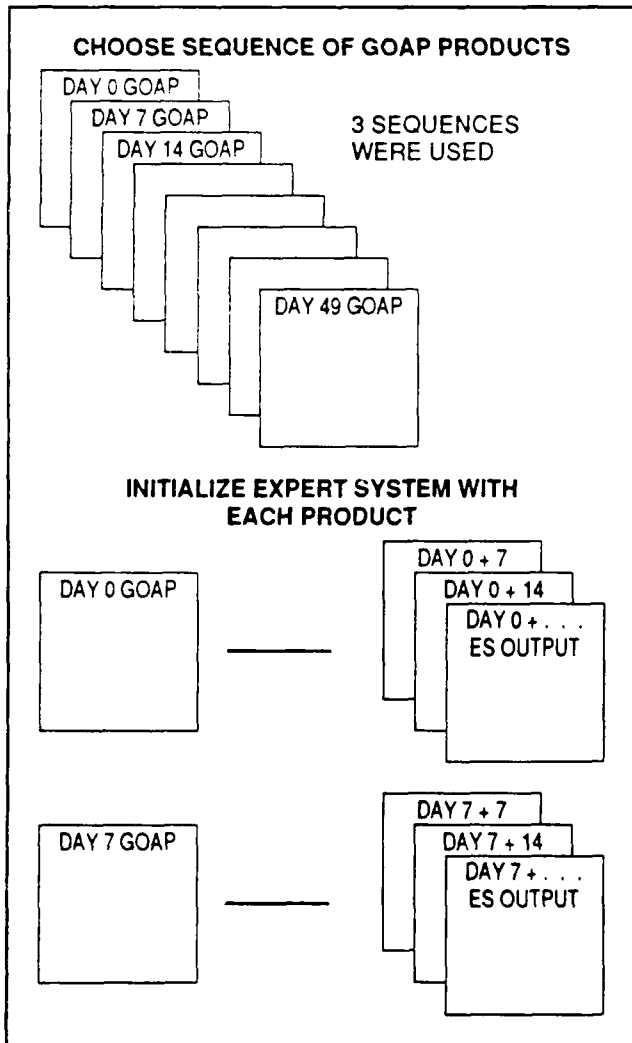
Figure 1. Expert system test plan (GOAP Data).
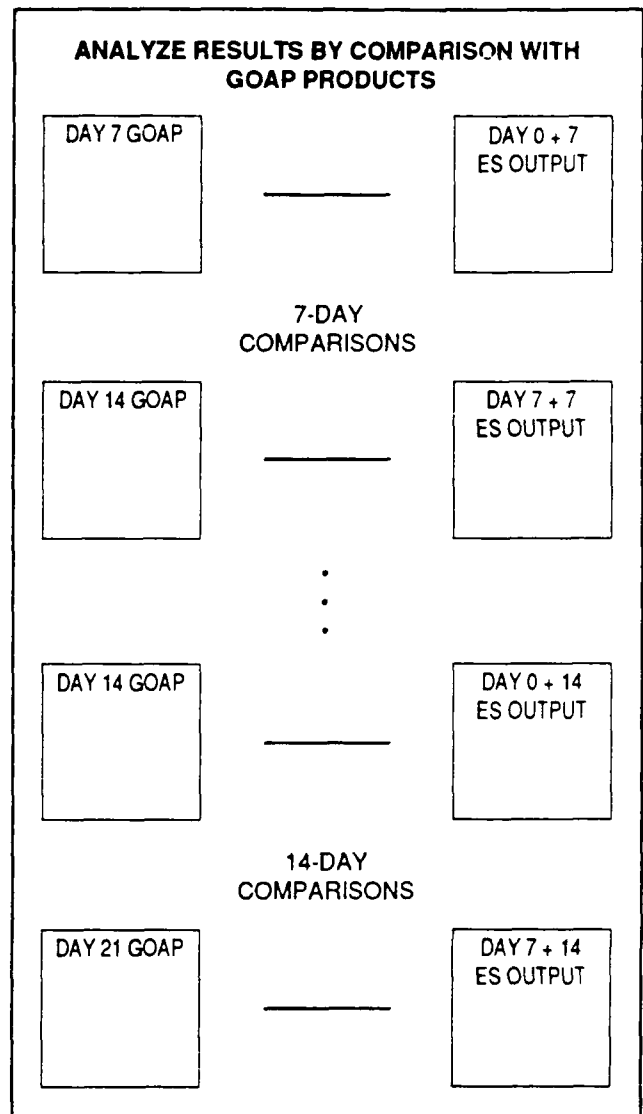
Figure 2. Expert system test results analysis (GOAP Data).

Table 1. Dates of GOAP mesoscale products used in expert system tests.

Sequence 1	Sequence 2	Sequence 3
86078	86332	86337
86085	86339	86344
86092	86346	86351
86099	86353	86357
86106	——	86365
86113	——	——
86120	87009	87014
86127	87016	——

The first two digits of each date indicate the year; the remaining three give the year-day number. There were enough winter products to create two overlapping sequences (2 and 3), with a few gaps. That situation did not exist for spring data; sequence 1 is the only spring sequence.

Table 2. Dates of Gulfcast and DART validation test data used in expert system tests.

Aug 85	Apr 87	Jul 87	May 88
85223	87098	87189	88125
85230	87105	87196	88132
	87112	87203	

The first two digits of each date indicate the year; the remaining three give the year-day number.

could have maximum possible confidence in the ocean truth derived from the GOAP analyses.

The second data set consisted of data also used to validate the Harvard Gulfcast model (Robinson et al., 1988) and an ocean nowcast/forecast system developed in the NOARL Data Assimilation Research and Transition (DART) program. Four sequences consisted of 10 dates, as shown in Table 2. The longest sequence was 14 days, so this data set could not be used to validate the expert system's performance for longer periods. However, this data set was particularly clean, so the quality of the comparisons should be very good.

3. Test Data Analysis

The analysis is based on comparisons between expert system output and ocean truth data. Each comparison involves one ring, whose identity is assumed to be maintained throughout the comparison. The requirements for a comparison are that a ring is present (1) in the initial state (ocean truth at day 0) data set at point P_1, (2) in the comparison (ocean truth at day N) data set at point P_2, and (3) in the expert system output (initial state propagated by the expert system) for day N at point P_3.

We have considered both scalar and vector error measures. The scalar measures are goodness of fit (GOF) values:

$$GOF_{translation} = d(P_2, P_3)/d(P_1, P_2) \qquad (1)$$

$$GOF_{size} = |1 - r(P_3)/r(P_2)| \qquad (2)$$

In these equations, $d(P_i, P_j)$ is the great-circle distance between P_i and P_j (see App. B), and $r(P_k)$ is the radius of the ring in the appropriate data set. Note that if $d(P_1, P_2) = 0$ (i. e., if the ring does not appear to move between the two ocean truth data sets), Eq. (1) cannot be applied to that comparison; the comparison must be discarded for translation.

Both GOF measures are formulated so that smaller values are "good," i. e., when the expert system values for day N are close to the corresponding ocean truth

values for day N, the values are small. Also, $GOF_{translation} = 1$ is the value the expert system would obtain if it "assumed" that the ring did not move at all. The latter observation provides a simple way to compare the expert system results with an assumption of no motion.

However, it may be reasonable to criticize $GOF_{translation}$ because it discards all information about the direction of the position errors. If some of the errors are in one direction and some are in the opposite direction, then one might conclude that, on the average, the expert system is doing fairly well. In this sense, $GOF_{translation}$ is an unduly pessimistic error measure. Also, if the true eddy positions are not precisely known (which they often are not in the GOAP products), Equation (1)'s denominator has substantial uncertainty. Since that denominator is likely to be small for the shorter times, the uncertainty in its value could lead to substantial errors. To first order, $|\Delta G| = [G/d(P_1, P_2)] \Delta d(P_1, P_2)$, where G is used as shorthand for $GOF_{translation}$. When $d(P_1, P_2)$ is small, $\Delta d(P_1, P_2)$ may actually be larger. In this case $|\Delta G| > G$, so the uncertainty predominates. Appendix B contains a numerical example that illustrates this situation.

A different view of the motion errors is provided by vector error measures. For one comparison, the position error for day N is resolved into components:

$$\Delta x = d(P_2, P_3) \sin \theta \qquad \Delta y = d(P_2, P_3) \cos \theta, \qquad (3)$$

where θ is the angle measured from the y (north-south) axis, conveniently obtained from spherical trigonometry. Δx is the east-west component and Δy is the north-south component; logic is applied to provide the correct sign (Δx is positive if P_3 is east of P_2, etc.). Once the vector errors are obtained for each comparison, then mean values of Δx and Δy for an entire data set, the magnitude of the mean vector error, and its direction can be obtained.

Together, the two types of motion-error measures provide a more complete picture than either one separately. The scalar measure gives information on the average magnitude of an error, while the vector errors help to indicate possible motion biases. Information of the latter type can be provided by inspecting both the individual vector errors and the mean vector error.

4. Test Results

We initialized the expert system with the three sequences listed in Table 1 and then ran each case for 7 weeks at 7-day intervals. A program bug prevented obtaining results for the runs initialized with the products

3

for days 86092, 86099, and 86106. The problem did not appear to affect any of the other cases. However, that situation severely limited the results for springtime data.

Appendix C lists the computer program that analyzed the expert system results and shows a sample of its output. That program examines the expert system output files (those files included the initial ring positions, as well as the hypothetical values for later times), finds matches for which the same ring is present in both the base and comparison data sets, and calculates the error measures defined by Equations (1)-(3). Subsequent calculations generate statistics from the individual results.

Table 3 lists a summary of overall scalar GOF results using GOAP mesoscale products. Most column headings require little or no explanation. "Pairs of data sets" refers to, e.g., (comparisons between) 86078-86085, 86337-86351, etc. Since $GOF_{translation} = 1$ is the "score" that an assumption of no motion would receive, "number compared to no motion" is easily found. "Number discarded" refers to the number of individual comparisons (rings) for which the ocean truth indicates that the ring did not move during the period under consideration. Then $d(P_1, P_2) = 0$, so Equation (1) cannot be evaluated. That situation actually occurred for a few 7- and 14-day comparisons, as Table 3 shows, and suggests the level of position uncertainty intrinsic to the GOAP products. The analysis program "flagged" the cases for which this occurred. Those comparisons were discarded only for $GOF_{translation}$; the other error measures were calculated. Finally, "mean fractional size error" refers to means of $GO._{site}^{-}$ over the groups listed.

Figures 3 and 4 plot some of the Table 3 data. Figure 3 shows "number compared to no motion" as the percentage of comparisons (excluding discarded comparisons) better than no motion. Figure 4 is a plot of mean fractional size error. "Days" labels the abscissas of both figures.

Table 4 lists overall mean values of the vector position errors. As is the case for Table 3, each entry is a statistic based on all the comparisons for the number of days given. Figures 5 and 6 show the same information in a different form. Each figure shows the mean vector error magnitude and direction versus number of days;

Table 3. Overall results based on scalar GOF values. GOAP mesoscale products and used as ocean truth.

Days	Pairs of Data Sets	Ring Type	Number Compared to NoMotion Better	Worse	Number Discarded	Mean Fractional Size Error
7	11	WCR	15	8	7	0.0376
		CCR	24	19	10	0.0285
		Total	39	27	17	0.0318
14	7	WCR	8	9	1	0.0625
		CCR	17	14	0	0.0452
		Total	25	23	1	0.0515
21	5	WCR	3	8	0	0.0598
		CCR	11	12	0	0.0643
		Total	14	20	0	0.0628
28	5	WCR	4	9	0	0.0821
		CCR	11	10	0	0.0844
		Total	15	19	0	0.0835
35	5	WCR	5	7	0	0.0892
		CCR	12	7	0	0.0794
		Total	17	14	0	0.0832
42	5	WCR	4	5	0	0.0812
		CCR	10	7	0	0.0532
		Total	14	12	0	0.0629
49	2	WCR	2	1	0	0.1030
		CCR	3	3	0	0.0710
		Total	5	4	0	0.0818
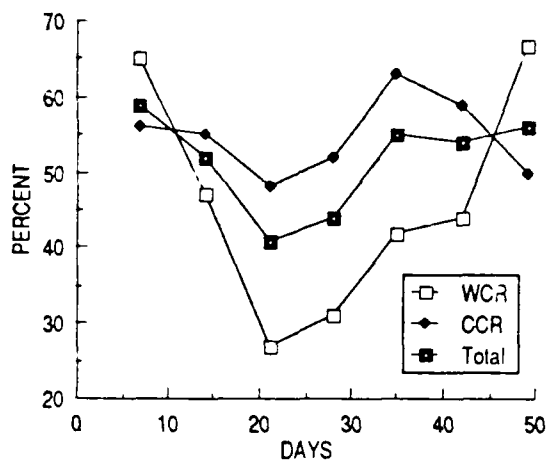
Figure 3. Percent of comparisons better than no motion (GOAP Data).

Figure 5. Mean vector position error—WCRs (GOAP Data).

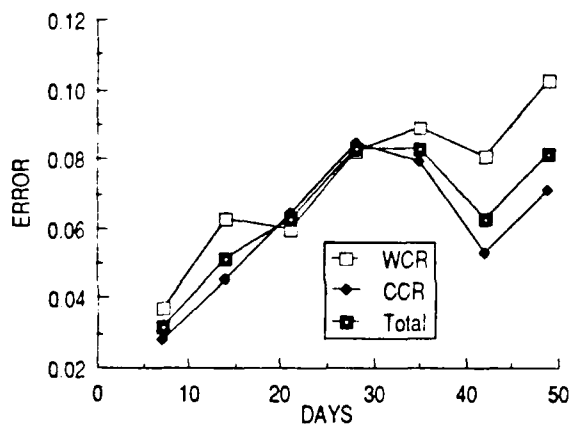*Figure 4. Mean fractional ring size error (GOAP Data).*
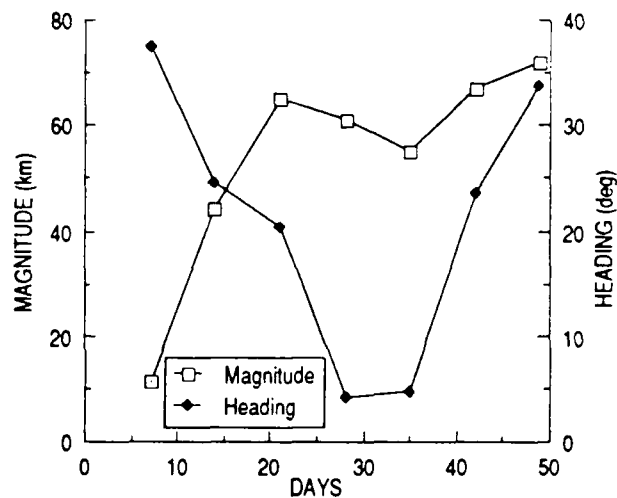
Figure 6. Mean vector position error—CCRs (GOAP Data).

Table 4. Mean vector error components (km). GOAP mesoscale products are used as ocean truth.

Days	WCRs		CCRs	
	Δx	Δy	Δx	Δy
7	-4.413	-0.9895	6.955	9.070
14	-28.89	-9.682	18.33	40.15
21	-72.03	-22.44	22.71	61.15
28	-62.07	-18.33	4.466	60.77
35	-60.82	-29.91	4.530	55.12
42	-91.09	-45.52	26.96	61.66
49	-84.63	-21.92	40.00	60.01

Figure 5 is for WCRs and Figure 6 is for CCRs. Direction is shown as a compass heading, with positive angles measured clockwise from north. Figure 7, which shows how many individual motion error vectors lie in each quadrant, provides a different view of those errors.

It is important to recall the dissimilarity in the way the different motion error measures are calculated. Both the scalar and vector measures involve the position "error" at the later time, i.e., the difference between where the expert system hypothesizes the ring will be located after a certain number of days and its (supposedly) true position then. The scalar data of Table 3 and Figure 3 are obtained by calculating a function (Eq. 1) of that error for each individual comparison and then averaging that function over some group (e.g., all warm rings for 21 days). All of the values of that function are nonnegative, which tends to increase the average. However, the vector error data (Table 4, Figs. 5 and 6) show averages of the errors themselves. Since the errors are distributed over all possible directions, they tend to compensate in the averages. So, the resulting averages show the extent to which the errors predominate in one direction.

Table 5 summarizes the overall scalar GOF results using Gulfcast and DART validation test data. It is similar to Table 3 for tests that use GOAP mesoscale

5

Table 5. Overall results based on scalar GOF values. Gulfcast and DART test, data are used as ocean truth.

Days	Pairs of Data Sets	Ring Type	Number Compared to No Motion Better	Worse	Number Discarded	Mean Fractional Size Error
7	6	WCR	19	12	1	0.0254
		CCR	25	14	0	0.0246
		Total	44	26	1	0.0250
14	2	WCR	6	5	0	0.0306
		CCR	10	5	0	0.0409
		Total	16	10	0	0.0366

DAYS	WCR		CCR		TOTAL	
7	8	4	18	15	26	19
	11	7	9	11	20	19
14	6	3	12	14	18	17
	7	2	2	3	9	5
21	4	1	6	12	10	13
	6	0	1	4	7	4
28	2	1	5	9*	7	10
	9	1	2	4	11	5
35	0	1	3	7	3	8
	10	1	4	5	14	6
42	0	0	3	7	3	7
	8	1	3	4	11	5
49	0	0	1	2	1	2
	3	0	1	2	4	2

*One CCR error was essentially along the negative (i.e., south) y axis.

Figure 7. Number of motion errors in each quadrant (GOAP Data).

Table 6. Mean vector error components (km). Gulfcast and DART test data are used as ocean truth.

Days	WCRs Δx	Δy	CCRs Δx	Δy
7	−9.487	−6.601	0.1611	4.216
14	−15.88	−10.20	2.481	12.56

products as ocean truth. However, there are no comparisons longer than 14 days because that is the longest sequence in the test data set.

Table 6 lists results analogous to those of Table 4, but for the Gulfcast and DART validation test data. The vector error results are similar to those obtained with the GOAP product data sets because WCR and CCR vector errors are each consistently in one quadrant, different for WCRs and CCRs, and the same quadrants as for the GOAP data sets. They are different in the sense that (except for WCR 7-day errors) they are smaller than the errors obtained with the GOAP data.

The magnitudes of the vector errors for each ring type increase with time. It is difficult to discern much else about trends in Tables 5 and 6 because the sequences are so short. Therefore, there are no plots similar to Figures 3-7 for the test results with the Gulfcast and DART data sets.

5. Discussion of Results

A. Tests Using GOAP Mesoscale Products

The previous section presented statistical summaries of the expert system test results. All of the error measures for the tests using GOAP products as ocean truth indicate somewhat similar behavior, increasing with

6

the number of days for a while, then essentially leveling off. Figure 3 shows that the worst results in comparison to an assumption of no motion occurred for 21 days. The mean vector error results shown in Figures 5 and 6 confirm this supposition; the errors barely increased after 21 days, while the actual distance a ring travels would normally be expected to increase moderately in most cases.

One of the basic statistical measures of time dependence is the linear trend. The linear trends indicated by the vector error statistics are as follows. For WCRs, the error increases 1.9 km/day, with heading $-110°$ (southwest). For CCRs, the error increases 1.1 km/day, with heading $30°$ (northeast). That is, these are the values of the magnitudes and directions of changes in the error vectors with time. These errors could be eliminated, *on the average*, by subtracting those motion vectors in all the ring motion rules. Also, the fractional size error increases by 0.0013 per day for WCRs, and by 0.0008 per day for CCRs.

As in any statistical study, the error sources and other factors that influence the statistics must be understood. One of the factors is that the number of comparisons decreases with increasing number of days; the figures for 49 days involve substantially fewer measurements than those for 7 days.

Counteracting that effect, at least for the scalar position GOF measure ($GOF_{translation}$), is the influence of imprecise position location in the GOAP mesoscale products. Ring positions in those products are sometimes determined from limited observational data, and are stated only to the nearest tenth of a degree of latitude and longitude. Consequently, a ring's actual motion during a short period may be less than the uncertainty in position in either of the GOAP products used to estimate that motion. A ring's "true" motion determined from GOAP products may be in error by more than 100% for the shorter periods (i. e., 7 or 14 days). This large percentage error can severely affect the accuracy of the $GOF_{translation}$ calculation. That, in turn, influences how many of those values are found to be better than no motion. The effect should be less pronounced for longer periods, when a ring moves farther. Likewise, the ring-size error measure has a "noise level" because ring sizes in the GOAP products are stated only to the nearest 5 nmi.

Appendix B's numerical example illustrates how position errors in the GOAP products can induce errors in the motion statistics. This problem does not completely invalidate the results for short periods, since errors of that type tend to cancel. However, it does increase the noise level. We can also extend the discussion of Appendix B to the vector position statistics. Both curves (WCRs and CCRs) rise sharply

at first, then substantially level off. The values for 7 and 14 days have high relative error because the position uncertainty in the two ring locations compared is the same order of magnitude as the distance between the locations. The trend shown by the remaining points of each curve can be interpreted as a bias (value for 0 days) related to the error in the starting position—which induces error in subsequent positions—and a slope due to error in the velocity vector used by the expert system. For WCRs this interpretation changes the trend vector to 0.86 km/day, with heading $-120°$. For CCRs the values become 0.82 km/day, with heading $-10°$. In both cases the bias is in the range of 50-60 km.

Individual rings are not identified in the GOAP products. We attached identifiers by visually inspecting the products in graphical form. Sometimes identification was difficult, particularly since the number of rings did not remain constant from product to product. In some cases a ring would disappear and then apparently reappear in a later product. (In such a case, e.g., a 7-day comparison would not be possible, but a 14- or 21-day comparison would.) It is possible that in some cases we made incorrect identifications. It is appealing to think that misidentification may account for some of the largest errors, but we must consider each such case individually. It may be best simply to eliminate ambiguous comparisons.

The greatest need, however, is for more high-quality data sets to serve as standards. The Gulfcast and DART validation test data set is one.

B. Tests Using Gulfcast and DART Validation Test Data

Trends are not as easy to establish for this data set as for the GOAP data because we only have results for 7 and 14 days. However, the results of "fitting" straight lines to the results are as follows:

- For CCRs, 1.0 km/day, heading $-120°$.
- For WCRs, 1.2 km/day, heading $20°$.

The fits are actually algebraic solutions that pass exactly through the data points; therefore, they retain all the uncertainty in those points. However, the biases are only in the range of 4-5 km (confirming the assumption that this data set is cleaner than the other), so the trend values are probably a reasonable reflection of the truth. Also, the fractional size error increases by 0.00074 per day for WCRs, and by 0.0023 per day for CCRs.

C. Overall Results

The corrected (with 7- and 14-day results removed) GOAP data set results are consistent with the Gulfcast

and DART data set results: For CCRs, error trends are approximately 1 km/day with heading approximately southwest; for WCRs, trends are (also) approximately 1 km/day, with heading approximately northeast. These mean vector errors should be removed from the rule base as a first attempt to upgrade the rules based on validation studies. The validation study should then be repeated after this adjustment to the rule base. Because many of the position errors will be reduced by this change, the scalar measure $GOF_{translation}$ is likely to be reduced, on the average. That, in turn, should improve the statistics on the percent of comparisons that are better than an assumption of no motion.

All of the statistics are overall values. We could separate the spring and winter (GOAP) data and compute separate values. However, there may not be enough data for statistical confidence, especially the spring data. We could also examine the data by regions to see whether the expert system rules for some regions give better results than rules for others. Again, there may not be enough data. We could look at individual comparisons, especially those with unusually large error measures. Doing so might identify rules that need modification. In some cases, it might also pinpoint cases for which the ocean truth has inaccurate values. Those cases, which may presently be biasing the statistics, could be eliminated.

The Remote Sensing Branch is continually seeking new data sets and will use them to continue the expert system evaluation. This evaluation, combined with other ongoing research efforts, will help to refine and improve the expert system rule base.

6. Summary

An oceanographic expert system with a knowledge base concerning mesoscale features in the Gulf Stream region of the North Atlantic is one knowledge-based tool the Remote Sensing Branch is developing to aid operational interpreters. The knowledge base concentrates on the time evolution of the features: warm-core and cold-core eddies and the Gulf Stream's north and south walls. This report summarizes the results of tests of the ring motion and size variation rules.

We used two data sets as ocean truth: a set consisting of three sequences of GOAP mesoscale products, and a smaller data set of analyses that were also used to evaluate the Harvard Gulfcast and NOARL DART models. The procedure was to initialize the expert system with one analysis, to evolve the expert system

forward in time, and to compare the evolved state with the analysis for the corresponding later date. The comparisons used scalar and vector ring-center position error measures, and a scalar ring-size error measure.

7. Conclusions

One overall result is that the expert system performs better with respect to ring motion than with an assumption of no motion for periods up to 14 days. This would not be the case, however, if the speeds or directions were seriously in error. The result is notable because a ring typically moves a distance less than half its diameter in 14 days, so an assumption of no motion is a good approximation for short periods. Also, ring-size errors are relatively small for several weeks. Examination of vector motion errors indicates systematic errors, so a simple approach to improvement would be to implement a gross correction for the average motion error in the ring motion data base. While this would improve the average results, individual ring motion might be seriously in error. *Recommendation: A detailed, case-by-case examination to identify specific problem areas is indicated.*

Some of the error indicated by the tests that used GOAP products as ocean truth is apparently due to errors and inaccuracy in those products themselves; some may also be due to errors in identifying a particular ring in products of different date. The fact that the number of rings in the GOAP products does not remain constant in time (creation or absorption of rings is generally not involved) magnifies the latter problem. Those factors limit the utility of the tests with the GOAP products. And, while the other (Gulfcast and DART) data set is of higher quality, it is a much smaller data set, and the longest sequence is only 14 days. *Recommendation: Identification of other data sets to use in testing the expert system is a high priority.*

8. References

Lybanon, M., J. D. McKendrick, R. E. Blake, J. R. B. Cockett, and M. G. Thomason (1986). A Prototype Knowledge-Based System to Aid the Oceanographic Image Analyst. *Applications of Artificial Intelligence III*, SPIE Vol. 635.

Lybanon, M., and R. L. Crout (1987). The NORDA GEOSAT ocean applications program. *Johns Hopkins APL Technical Digest* 8(2):212-218.

Robinson, A. R., M. A. Spall, and N. Pinardi (1988). Gulf stream simulations and the dynamics of ring

and meander processes. *Journal of Physical Oceanography* 18:1811-1853.

Thomason, M. G. and R. E. Blake (1986). *Development of an Expert System for Interpretation of Oceanographic Images.* Naval Ocean Research and Development Activity, Stennis Space Center, MS. NORDA Report 148.

Thomason, M. G. (1987). *Oceanographic Expert System Development Final Report—Year 1.* Prepared for NORDA under Contract No. N00014-87-C-6001, November.

Tracey, K. L. and D. R. Watts (1986). On Gulf Stream meander characteristics near Cape Hatteras. *Journal of Geophysical Research* 91(C6):7587-7602.

Appendix A

Rule Base Details

The prototype oceanographic expert system depicts expected motions and size changes of warm-core rings (WCR) and cold-core rings (CCR), and their interactions, both with each other and with the Gulf Stream, in different regions of the northwest Atlantic Ocean. The domain is divided into nine regions, primarily based on longitude. (More details are given in Lybanon (1988), NTN 368). The rules that describe the expected behavior of WCRs and CCRs differ in each region.

In each time step, each ring has its position and size updated. That operation is followed by a determination of the ring's interaction with the Gulf Stream; the interaction is determined by the distance and direction of the center of the ring to the nearest point on the Gulf Stream boundary. The interaction may also affect the ring's motion. Because of the importance of the ring-Gulf Stream interaction, the expert system also simulates Gulf Stream motion.

Table A1 lists the basic ring motion parameters for the nine regions. The situation is considerably more complicated when a ring is close enough to the Gulf Stream for the interaction rules to come into play. As an example, the next several tables summarize the "Gulf Stream interaction" motion rules for CCRs in region 5.

Behavior is based on the ratio of the ring's radius to its distance of closest approach to the Gulf Stream. Three interaction regimes are defined by this ratio and are specified by "breakpoints." The details in the first two regimes depend on the ring's direction of motion, as specified by a number in the range 1-16, where direction 1 is due north and the others proceed clockwise in sixteenths of a revolution.

Table A2 gives the ring's behavior in the first interaction regime. Latitude and longitude factors multiply a distance based on the speed given in Table A1 and the time step, thereby specifying the motion. It is necessary to note that west longitudes are positive in the expert system. The last column in Table A2 lists the changes to the direction numbers.

In the second interaction regime (closer to the Gulf Stream) motion is based on a higher speed—2 cm/sec faster than the nominal value. Also, if the ring has had a Gulf Stream "encounter" (signified by a negative DIR) the ring's radius is increased by 10% and the sign of DIR is made positive. Table A3, similar to A2, specifies the resulting motion in the second interaction regime.

Table A1. Ring motion parameters when there is no Gulf Stream interaction.

Region	WCRs Speed (cm/sec)	WCRs Heading (deg)	CCRs Speed (cm/sec)	CCRs Heading (deg)
1	8.0*	0*	6.0	−93
2	8.0	−150	6.0	−112
3	8.0	−120	6.0	−67
4	6.0	−100	6.0	−100
5	7.5	−116	5.0	−96
6	6.0	−112	5.0	−96
7	5.0	−96	5.0	−96
8	5.0	−93	5.0	−96
9	5.0	−92	5.0	−96

*No WCRs are expected in region 1.

Table A2. Cold-core ring motion parameters for region 5, interaction regime 1.

Initial DIR	Latitude Factor	Longitude Factor	ΔDIR
1, 2	0.985	−0.174	0
3, 4	0.866	−0.500	+1
5, 6	−0.985	−0.174	+1
7, 8	−0.866	−0.500	+1
9, 10	−1.0	0	+1
11, 12	−0.707	0.707	+1
13, 14	0.994	0.104	+1
15, 16	0.707	0.707	0

13

Table A3. CCR motion parameters for region 5, interaction regime 2.

Initial DIR	Latitude Factor	Longitude Factor	Final DIR
1, 2	0.500	−0.300	3
3, 4	−0.500	−0.100	5
5, 6	−0.700	0.100	7
7, 8	−0.400	0.400	9
9, 10	−0.104	0.995	11
11, 12	0.104	0.995	13
13, 14	0.500	0.866	15
15, 16	0.927	0.385	1

Table A4. Cold-core ring motion parameters for region 5, interaction regime 3.

Ring to GS* Direction	Latitude Factor	Longitude Factor	Final DIR
1	−0.707, −0.400	−0.500, −0.400	−7
3	−0.707, −1.0	−0.707, 0	−8
5	−1.0 , −0.500	0 , 0.500	−10
7	−0.500, −0.438	0.707, 0.898	−12
9	0.707, 0.500	0.707, 0.866	−14
11	0.707, 0.994	0.707, 0.104	−16
13	0.707, 0.438	−0.438, −0.400	−2
15	0.300, −0.200	−0.400, 0	−5

The first entry of each pair in the latitude and longitude factors columns is the value used if there was no immediately previous encounter (DIR > 0), while the second is the value used if there was (DIR < 0).
*GS = Gulf Stream

The third interaction regime (closest to the Gulf Stream) is where the fastest movement and "encounters" with the Gulf Stream take place. In this regime the details depend on the direction of the ring to Gulf Stream projection vector. Also, they depend on whether the ring has already had an encounter (DIR < 0) or not (DIR > 0). Also, motion is based on a speed 4 cm/sec faster than the nominal value. Table A4 lists the numerical values.

Finally, the region parameters follow. Those parameters include ring-size decay factors and values used in Gulf Stream interaction tests, as well as the basic ring-motion parameters. Note that the "lat adjust" and "long adjust" factors are direction cosines.

Appendix A Reference

Lybanon, M. (1988). *Oceanographic Expert System Functional Description.* Naval Ocean Research and Development Activity, Stennis Space Center, MS, NORDA Technical Note 368.

Appendix B

Geometrical Equations and Numerical Example

The great circle distance between two points on a sphere, P_A and P_B, can be found easily from one of the formulas for the solution of spherical triangles (Abramowitz and Stegun, 1970). Consider the spherical triangle with one vertex at the north pole: one at P_A and one at P_B. Then designate d as the great circle arc connecting P_A and P_B. Thus, the angle at the north pole vertex opposite d is $\lambda_A - \lambda_B$, and

$$\cos d = \cos (90 - \phi_A) \cos (90 - \phi_B)$$
$$+ \sin (90 - \phi_A) \sin (90 - \phi_B) \cos (\lambda_A - \lambda_B)$$
$$= \sin \phi_A \sin \phi_B + \cos \phi_A \cos \phi_B \cos (\lambda_A - \lambda_B). \tag{B1}$$

In this equation, ϕ and λ are latitude and longitude, respectively. The arc d can be converted to a distance by multiplying it by 6378 km, the approximate WGS-84 semimajor axis, treated as the radius of a spherical earth here. Eq. (B1) gives the d values used in Eqs. (1) and (3). Another useful spherical triangle formula from Abramowitz and Stegun is

$$\sin A/\sin a = \sin B/\sin b = \sin C/\sin c, \tag{B2}$$

where A, B, and C are the three vertex angles and a, b, and c are the opposite sides.

The use of Eqs. (B1) and (B2) clearly illustrates the problem introduced into Eq. (1), the scalar motion goodness-of-fit (GOF) measure, by inaccuracy in the knowledge of the ring positions in the ocean truth data sets. The problem is most severe for shorter periods, when the true ring motion is relatively small.

Suppose that the true (but unknown) values of a set of ocean truth ring positions are $P_1 = (40.44 \text{ N}, 63.36 \text{ W})$ and $P_2 = (40.25 \text{ N}, 63.61 \text{ W})$. The supposed values obtained from the ocean truth data sets will not be quite these, for several reasons. The along-track altimeter resolution is about 7 km and the resolution of the satellite imagery used is 5 km. A ring's boundary can only be determined to within a few altimeter samples, and the track will not in general pass directly over the ring's center. Cloud cover typically interferes with the satellite imagery, which again leads to some error in determining the ring's location. Also, the analyst rounds off to 0.1 degree in latitude and longitude. Because of all these factors, suppose that the ring positions given in the two ocean truth data sets are $P_1^{truth} = (40.3 \text{ N}, 63.4 \text{ W})$ and $P_2^{truth} = (40.3 \text{ N}, 63.5 \text{ W})$. This corresponds to location errors of 15.9 km and 10.9 km, respectively, which are not unreasonable.

Assume that the expert system starts with P_1^{truth} and "moves" the ring to $P_3 = (40.166 \text{ N}, 63.576 \text{ W})$. This corresponds to about 21 km to the southwest, a reasonable value for a week's motion. Then, from Eq. (B1),

$$d = 8.4898 \text{ km}, \qquad \Delta d = 16.255 \text{ km}, \tag{B3}$$

and Eq. (1) gives:

$$GOF_{translation} = 1.915. \tag{B4}$$

This value is almost twice what an assumption of no motion would give. But if the true values of P_1 and P_2 are used, then we would have

$$d = 29.953 \text{ km}. \tag{B5}$$

Since this goes into the denominator of Eq. (1), clearly this value of d will yield a very different value for $GOF_{translation}$ than the value in Eq. (B3). Now, Δd will also change. Starting with the true P_1, the expert system will give $P_3 = (40.306 \text{ N}, 63.536 \text{ W})$, which results in

$$\Delta d = 8.8518 \text{ km} \quad [\underline{smaller} \text{ than before}] \tag{B6}$$

and

$$GOF_{translation} = 0.296. \tag{B7}$$

This is substantially better than the value that an assumption of no motion would give. So, this numerical example clearly indicates that position uncertainties in the ocean truth data sets could have a significant impact on the motion statistics for shorter periods. In another case the change might be in the opposite direction. For longer times, when d and Δd are greater relative to the uncertainties in their assumed values, this problem has less effect on the motion statistics.

Appendix B References

Abramowitz, M., and I. A. Stegun, eds. (1970). *Handbook of Mathematical Functions With Formulas, Graphs, and Mathematical Tables*. National Bureau of Standards, Applied Mathematics Series, Number 55, Ninth Printing.

Appendix C

Analysis Program Listing and Sample Output

```
WREG1 8.0 1   1.0      0.0 0.5 100. 0. .9 .75 .5
WREG2 8.0 9  -0.866 +0.500 0.9 30. 0.8      .9 .75 .5
WREG3 8.0 10 -0.500 +0.866 0.95 30. 0.85    .9 .75 .5
WREG4 6.0 12 -0.174 +0.985 0.99 35. 0.96    .9 .75 .5
WREG5 7.5 11 -0.438 +0.898 0.998 30. 0.98    .9 .75 .5
WREG6 6.0 12 -0.358 +0.927 0.998 30. 0.98    .9 .75 .5
WREG7 5.0 13 -0.104 +0.994 0.999 30. 0.98    .9 .75 .5
WREG8 5.0 13 -0.052 +0.998 0.999 35. 0.98    .9 .75 .5
WREG9 5.0 13 -0.035 +0.999  0.999 35. 0.98   .9 .75 .5
CREG1 6.0 10 -0.052 +0.998 0.998    25. 0.8     0.3 0.31 0.8 0.
CREG2 6.0 10 -0.358 +0.927 0.998 25. 0.9     0.3 0.31 0.8 0.
CREG3 6.0 7  +0.385 +0.927 0.998 25.0 0.9      0.3 0.31 0.8 0.
CREG4 6.0 10 -0.174 +0.985 0.999 25. 0.95     0.3 0.31 0.8 0.
CREG5 5.0 11 -0.104 +0.994 0.999 25. 0.95     0.3 0.31 0.8 0.
CREG6 5.0 11 -0.104 +0.994 0.999 30. 0.95    0.3 0.31 0.8 0.
CREG7 5.0 11 -0.104 +0.994 0.9999 35. 0.98     0.3 0.31 0.8 0.
CREG8 5.0 12 -0.104 +0.994 0.9999 35. 0.98   0.75 0.751 0.9 0.
CREG9 5.0 13 -0.104 +0.994 0.9999 35. 0.98   0.75 0.751 0.95 0.
```

Items per line are region name, speed (cm/sec), direction (one of 16
for general reference), lat adjust factor, long adjust, decay when not
in GSinteract, min radius for no coalesce with GS, decay in GSinteract.

For wcregions, also breakpoints b1-3 for ratio tests in GSinteraction.

For ccregions, also breakpoints b1-4 for ratio tests for looping effects.

```c
/*  Program to analyze oceanographic expert system test results  */
/*       DEBUG PRINT STATEMENTS ADDED 3/3/89         */
#include <stdio.h>
#include <math.h>
#define REARTH 6378   /*  WGS-84 semimajor axis in km  */
#define DEGRAD 0.01745329252  /*  pi/180  */
main ()
{
    int ncases, ndays, i, j, k, l, day, nbid, ncid, match, matchn;
    float lat[3], lon[3], rad[3];
    char base[15], comp[15], rid[10];
    char debugyn[15];
    int dbg;
    float latb0[20], lonb0[20], radb0[20];
    float latbn[20], lonbn[20], radbn[20];
    float latc0[20], lonc0[20], radc0[20];
    double d, deltad, deltax, deltay, theta, goftrans, gofsize;
    char ridb0[20][10], ridbn[20][10], ridc0[20][10];
    FILE *fopen(), *fpin, *fpout, *fpb, *fpc;
    fpin = fopen ("ESANAL.DAT", "r");
    fscanf (fpin, "%d %d %s", &ncases, &ndays, &debugyn[0]);
    if (strcmp (&debugyn[0], "DEBUG") == 0)
        dbg = 1;
    else
        dbg = 0;
    fpout = fopen ("ESANAL.OUT", "w");
    fprintf (fpout, "\f\tEXPERT SYSTEM RESULTS FOR %d DAYS\n", ndays);
    for (i=1; i<=ncases; i++)  /*  Loop on cases  */
    {
        fscanf (fpin, "%s %s", &base[0], &comp[0]);
        fpb = fopen (base, "r");
        fpc = fopen (comp, "r");
/*  Load information from test output files  */
```

```c
/*      Get day 0 information from base file  */
        day = findday (fpb);  /*  Day number  */
        if (day != 0)
        {
            printf ("\nDay 0 data not at beginning of base file.");
            exit ();
        }
        j = 0;
        while (fscanf (fpb, "%s %f %f %f",
            &ridb0[j][0], &latb0[j], &lonb0[j], &radb0[j]) == 4)
            j++;
        nbid = j;  /*  Number of ring identifiers in base file.  */
/*      Get day 0 information from comparison file  */
        day = findday (fpc);  /*  Day number  */
        if (day != 0)
        {
            printf ("\nDay 0 data not at beginning of comparison file.");
            exit ();
        }
        j = 0;
        while (fscanf (fpc, "%s %f %f %f",
            &ridc0[j][0], &latc0[j], &lonc0[j], &radc0[j]) == 4)
            j++;
        ncid = j;  /*  Number of ring identifiers in comparison file  */
/*      Get day ndays information from comparison file  */
```

```c
        while (day<ndays) day = findday (fpb);
/*                      day>= ndays  */
        if (day == 9999)
        {
            printf ("\nEOF encountered in base file ");
            printf ("while searching for day %d data.", ndays);
            exit ();
        }
        if (day > ndays)
        {
            printf ("\nDay %d data not in base file.", ndays);
            exit ();
        }
/*  Found it!  */
        for (j=0; j<nbid; j++)  /*  Loop on ring IDs in base file  */
            fscanf (fpb, "%s %f %f %f",
                &ridbn[j][0], &latbn[j], &lonbn[j], &radbn[j]);
/*  Close files.  */
        fclose (fpb);
        fclose (fpc);
/*  Print file name header.  */
        fprintf (fpout, "\n\n\nBase:        %s", base);
        fprintf (fpout,    "\nComparison: %s", comp);
if (dbg) fprintf (fpout, "\nDEBUG     nbid = %d     ncid = %d",
                nbid, ncid); /* D */
/*  Loop over IDs in base file.  */
        for (j=0; j<nbid; j++)
        {
            strcpy (&rid[0], ridb0+j);
if (dbg) fprintf (fpout, "\nDEBUG base file ring ID is %s", rid); /* D */
/*  Is the same ring ID in the comparison file?  */
            for (match=0, k=0; ((match==0)&&(k<ncid)); k++)
            {
                if (strcmp (&rid[0], ridc0+k) == 0) match = 1;
if (dbg)
            {fprintf (fpout, "\nDEBUG     comp. file ring ID is %s",
                *(ridc0+k)); /* D */
            fprintf (fpout, "\nDEBUG      k = %d     match = %d",
                k, match);} /* D */
```

22

```c
                }
            if (match==1)
            {  /*  Ring ID is in comparison file.  */
                k--;
                lat[0] = latb0[j] * DEGRAD;
                lon[0] = lonb0[j] * DEGRAD;
                lat[1] = latc0[k] * DEGRAD;
                lon[1] = lonc0[k] * DEGRAD;
                rad[1] = radc0[k];
/*  Find position in base file data set, day ndays.  */
if (dbg) fprintf (fpout, "\nDEBUG looking for %s in base file, day %d",
                rid, ndays);
                for (matchn=0, l=0; ((matchn==0)&&(l<nbid)); l++)
                    {
                    if (strcmp (&rid[0], ridbn+l) == 0) matchn = 1;
if (dbg)
        {fprintf (fpout, "\nDEBUG    ring ID is %s", *(ridbn+l)); /* D */
         fprintf (fpout, "\nDEBUG    for l = %d, matchn = %d",
                l, matchn);} /* D */
```

```c
                    }
                if (matchn!=1)
                {
                    printf ("\nRing id %s not in base file for day %d.",
                        rid, ndays);
                    exit();
                }
if (dbg)
        {fprintf (fpout, "\nDEBUG found in base file for day %d",
                ndays); /* D */
         fprintf (fpout, "\nDEBUG    position %d", l);} /* D */
                l--;
                lat[2] = latbn[l] * DEGRAD;
                lon[2] = lonbn[l] * DEGRAD;
                rad[2] = radbn[l];
if (dbg)
        {fprintf (fpout, "\nDEBUG Comparing j = %d,   k = %d,   l = %d",
                j, k, l); /* D */
         fprintf (fpout, "\nDEBUG    Ring IDs   %s        %s        %s",
                rid, *(ridc0+k), *(ridbn+l));} /* D */
/*  Calculate  */
                process_one_comparison (rid, lat, lon, rad, &d, &deltad,
                    &deltax, &deltay, &theta, &goftrans, &gofsize, fpout);
            }  /*  End ring ID in comparison file sequence.  */
        }  /*  End loop on ring IDs in base file.  */
    }  /*  End loop on cases.  */
/*  Global statistics calculation section goes here.  */
}
/*  Function to find day-number header for block of data in file fp  */
findday (fp)
FILE *fp;
{
    int c, day;
    while ((c = getc(fp)) != ':');          /*  Locate colon.  */
    if (fscanf (fp, "%d", &day) == EOF)
        return 9999;
    else
        return day;  /*  Day number  */
}
/*  Function to calculate goodness-of-fit measures for one pair.  */
process_one_comparison (rid, lat, lon, rad, dist, ddist, dx, dy, th,
                        goft, gofs, fpout)
char rid[];
float lat[], lon[], rad[];
double *dist, *ddist, *dx, *dy, *th, *goft, *gofs;
FILE *fpout;
```

23

```c
{
    double lat1, lon1, lat2, lon2, lat3, lon3, rad2, rad3, ang_d, ang_dd, thd;
/*  Calculate great circle distance and angle  */
/*  between base (day 0) and comparison values.  */
    lat1 = lat[0];
    lon1 = lon[0];
    lat2 = lat[1];
    lon2 = lon[1];
    scaldist (lat1, lon1, lat2, lon2, dist, &ang_d);
/*  Calculate great circle distance and angle  */
/*  between comparison and base (day ndays) values.  */
    lat3 = lat[2];
```

```c
    lon3 = lon[2];
    scaldist (lat2, lon2, lat3, lon3, ddist, &ang_dd);
/*  Calculate goodness of fit (translation).  */
    goftrans (*ddist, *dist, goft);
/*  Calculate vector errors between base and comparison positions  */
/*  for day ndays.  */
    vecterrs (lat2, lon2, lat3, lon3, *ddist, ang_dd, dx, dy, th);
/*  Calculate goodness of fit (size).  */
    rad2 = rad[1];
    rad3 = rad[2];
    gofsize (rad2, rad3, gofs);
/*  Print results.  */
    fprintf (fpout, "\n\n\tRing %s", rid);
    fprintf (fpout, "\nG. o. f. (trans) = %f", *goft);
    fprintf (fpout, "\nG. o. f. (size)  = %f", *gofs);
    thd = (*th) / DEGRAD;  /*  angle in degrees  */
    fprintf (fpout, "\ndeltax = %f km    deltay = %f km    theta = %f deg",
             *dx, *dy, thd);
}
/*  Now for the good stuff!  */
/*  CALCULATIONS  */
/*  All angles in radians.  All distances in kilometers.  */
/*  Function to calculate great circle scalar distances  */
scaldist (lata, lona, latb, lonb, dist, ang_d)
double lata, lona, latb, lonb;
double *dist, *ang_d;
{
    double cosd;
    cosd = sin (lata) * sin (latb) +
           cos (lata) * cos (latb) * cos (lona - lonb);
    cosd = fabs (cosd);  /*  Magnitude  */
    *ang_d = acos (cosd);
    *dist = REARTH * (*ang_d);
}
/*  Function to calculate the goodness of fit for translation  */
goftrans (ddist, dist, goft)
double ddist, dist, *goft;
{
    if (dist)
        *goft = ddist / dist;  /*  Always >= 0.  */
    else
        *goft = -1;  /*  Implies zero reference motion (dist).  */
}
/*  Function to calculate vector errors between base and comparison  */
/*  ring positions  */
vecterrs (lata, lona, latb, lonb, ddist, ang_dd, dx, dy, th)
double lata, lona, latb, lonb, ddist, ang_dd, *dx, *dy, *th;
{
    double sinth, costh;
    if (fabs (ang_dd) < 8.7e-4)
        sinth = 0.;  /*  Points coincide  */
    else
```

24

```c
    sinth = (cos (latb) * sin (fabs (lona - lonb)) / sin (ang_dd));
    *th = asin (sinth);
    costh = cos (*th);
/*  Calculate E component.  */
    *dx = ddist * sinth;
    if (lonb>lona) *dx = -(*dx);
```

```c
/*  Calculate N component.  */
    *dy = ddist * costh;
    if (latb<lata) *dy = -(*dy);
}
/*  Function to calculate the goodness of fit for size  */
gofsize (rad2, rad3, gofs)
double rad2, rad3, *gofs;
{
    *gofs = fabs (1 - (rad3 / rad2));
}
```

          EXPERT SYSTEM RESULTS FOR 14 DAYS

Base: UTK86113.OUT
Comparison: UTK86127.OUT

        Ring WCR2
G. o. f. (trans) = 0.632428
G. o. f. (size) = 0.089539
deltax = 21.356864 km   deltay = -61.139292 km   theta = 19.255068 deg

        Ring WCR3
G. o. f. (trans) = 0.997614
G. o. f. (size) = 0.003996
deltax = -27.868062 km   deltay = -0.459515 km   theta = 89.055339 deg

        Ring WCR4
G. o. f. (trans) = 0.246814
G. o. f. (size) = 0.119380
deltax = -6.133347 km   deltay = -5.508179 km   theta = 48.073918 deg

        Ring CCR6
G. o. f. (trans) = 1.268131
G. o. f. (size) = 0.051899
deltax = 79.221727 km   deltay = 175.105664 km   theta = 24.343062 deg

        Ring CCR7
G. o. f. (trans) = 0.997710
G. o. f. (size) = 0.020196
deltax = 147.656794 km   deltay = 53.644116 km   theta = 70.033779 deg

Base: UTK86332.OUT
Comparison: UTK86346.OUT

        Ring WCR1
G. o. f. (trans) = 2.771150
G. o. f. (size) = 0.182477
deltax = -57.265707 km   deltay = -33.118660 km   theta = 59.957779 deg

        Ring WCR2
G. o. f. (trans) = 0.480591
G. o. f. (size) = 0.062856
deltax = -12.115247 km   deltay = -19.749530 km   theta = 31.526820 deg

```
        Ring CCR1
G. o. f. (trans) = 3.144583
G. o. f. (size)  = 0.119380
deltax = -19.598384 km    deltay = 64.106701 km    theta = 16.999181 deg


        Ring CCR2
G. o. f. (trans) = 0.745550
G. o. f. (size)  = 0.002000
deltax = 114.393046 km    deltay = 20.323103 km    theta = 79.925927 deg


        Ring CCR3
G. o. f. (trans) = 0.411050
```

```
G. o. f. (size)  = 0.000198
deltax = 28.550786 km    deltay = 5.671743 km    theta = 78.764211 deg


        Ring CCR4
G. o. f. (trans) = 0.371599
G. o. f. (size)  = 0.000200
deltax = 2.334919 km    deltay = -16.641101 km    theta = 7.987051 deg


        Ring CCR5
G. o. f. (trans) = 0.789832
G. o. f. (size)  = 0.121397
deltax = -2.167645 km    deltay = 38.059487 km    theta = 3.259709 deg


Base:         UTK86339.OUT
Comparison:   UTK86353.OUT


        Ring WCR1
G. o. f. (trans) = 1.178608
G. o. f. (size)  = 0.019900
deltax = -31.171101 km    deltay = 11.261030 km    theta = 70.136983 deg


        Ring WCR2
G. o. f. (trans) = 1448363.280568
G. o. f. (size)  = 0.027279
deltax = -48.021978 km    deltay = 7.899019 km    theta = 80.659199 deg


        Ring WCR3
G. o. f. (trans) = 0.486439
G. o. f. (size)  = 0.023916
deltax = 39.989666 km    deltay = -11.537413 km    theta = 73.906627 deg


        Ring CCR1
G. o. f. (trans) = 6.617396
G. o. f. (size)  = 0.119380
deltax = -28.700930 km    deltay = 52.999620 km    theta = 28.436912 deg


        Ring CCR2
G. o. f. (trans) = 0.633112
G. o. f. (size)  = 0.191161
deltax = 43.009360 km    deltay = 30.798889 km    theta = 54.393649 deg


        Ring CCR3
G. o. f. (trans) = 1.398357
G. o. f. (size)  = 0.039793
deltax = 38.820212 km    deltay = 28.711605 km    theta = 53.513202 deg


        Ring CCR4
G. o. f. (trans) = 1.185326
G. o. f. (size)  = 0.000200
deltax = -23.932959 km    deltay = 5.657029 km    theta = 76.701094 deg
```

```
        Ring CCR5
G. o. f. (trans) = 1.515371
G. o. f. (size)  = 0.000200
deltax = -32.003549 km     deltay = 16.819605 km     theta = 62.275633 deg
```

Base: UTK86337.OUT
Comparison: UTK86351.OUT

```
        Ring WCR1
G. o. f. (trans) = 1.178608
G. o. f. (size)  = 0.019900
deltax = -31.171101 km     deltay = 11.261030 km     theta = 70.136983 deg

        Ring WCR2
G. o. f. (trans) = 4.714671
G. o. f. (size)  = 0.027279
deltax = -39.490286 km     deltay = 7.850004 km     theta = 78.757121 deg

        Ring CCR1
G. o. f. (trans) = 3.141976
G. o. f. (size)  = 0.119380
deltax = -19.622385 km     deltay = 64.107054 km     theta = 17.018708 deg

        Ring CCR2
G. o. f. (trans) = 0.781846
G. o. f. (size)  = 0.002000
deltax = 123.308899 km     deltay = 31.576990 km     theta = 75.636341 deg

        Ring CCR3
G. o. f. (trans) = 1.343808
G. o. f. (size)  = 0.020198
deltax = 39.248147 km     deltay = 86.733713 km     theta = 24.347378 deg

        Ring CCR4
G. o. f. (trans) = 0.789366
G. o. f. (size)  = 0.000200
deltax = -15.220582 km     deltay = -16.627240 km     theta = 42.470998 deg

        Ring CCR5
G. o. f. (trans) = 2.208780
G. o. f. (size)  = 0.121397
deltax = -36.359242 km     deltay = 38.145244 km     theta = 43.626784 deg
```

Base: UTK86344.OUT
Comparison: UTK86357.OUT

```
        Ring WCR1
G. o. f. (trans) = -1.000000
G. o. f. (size)  = 0.096739
deltax = -48.488118 km     deltay = -10.914194 km     theta = 77.314704 deg

        Ring WCR2
G. o. f. (trans) = 3.663607
G. o. f. (size)  = 0.066855
deltax = -49.374569 km     deltay = 14.341100 km     theta = 73.803787 deg

        Ring WCR3
G. o. f. (trans) = 0.632485
G. o. f. (size)  = 0.023916
deltax = 82.502777 km     deltay = 22.201190 km     theta = 74.938697 deg

        Ring CCR1
```

27

G. o. f. (trans) = 2.155328
G. o. f. (size) = 0.001999
deltax = -10.580226 km   deltay = 75.223236 km   theta = 8.006191 deg

          Ring CCR2
G. o. f. (trans) = 1.784784
G. o. f. (size) = 0.002000
deltax = -1.509890 km   deltay = 75.216759 km   theta = 1.149992 deg

          Ring CCR3
G. o. f. (trans) = 1.200311
G. o. f. (size) = 0.039793
deltax = 60.079620 km   deltay = 43.044195 km   theta = 54.380200 deg

          Ring CCR4
G. o. f. (trans) = 0.489840
G. o. f. (size) = 0.000200
deltax = 19.863945 km   deltay = 27.909121 km   theta = 35.440852 deg

          Ring CCR5
G. o. f. (trans) = 0.136847
G. o. f. (size) = 0.000200
deltax = 2.283161 km   deltay = 5.621360 km   theta = 22.104934 deg

Base: UTK86351.OUT
Comparison: UTK86365.OUT

          Ring WCR1
G. o. f. (trans) = 0.561618
G. o. f. (size) = 0.028328
deltax = 11.810216 km   deltay = 44.602242 km   theta = 14.830970 deg

          Ring WCR2
G. o. f. (trans) = 1.649121
G. o. f. (size) = 0.098467
deltax = -30.983492 km   deltay = 13.097733 km   theta = 67.084634 deg

          Ring WCR3
G. o. f. (trans) = 0.481292
G. o. f. (size) = 0.093684
deltax = 31.532682 km   deltay = 32.948683 km   theta = 43.741995 deg

          Ring CCR1
G. o. f. (trans) = 0.398355
G. o. f. (size) = 0.205891
deltax = 30.738149 km   deltay = -11.012940 km   theta = 70.288288 deg

          Ring CCR2
G. o. f. (trans) = 0.878067
G. o. f. (size) = 0.042910
deltax = -82.694382 km   deltay = -14.792261 km   theta = 79.858270 deg

          Ring CCR3
G. o. f. (trans) = 1.062258
G. o. f. (size) = 0.020198
deltax = 86.098359 km   deltay = 66.718503 km   theta = 52.227528 deg

          Ring CCR4
G. o. f. (trans) = 0.706672
G. o. f. (size) = 0.000200
deltax = 89.989516 km   deltay = 39.510746 km   theta = 66.295671 deg

```
        Ring CCR5
G. o. f. (trans) = 0.710231
G. o. f. (size) = 0.000200
deltax = 79.646098 km     deltay = -38.494162 km     theta = 64.204820 deg


Base:        UTK86365.OUT
Comparison:  UTK87014.OUT

        Ring WCR2
G. o. f. (trans) = 1.471350
G. o. f. (size) = 0.096740
deltax = -150.977189 km     deltay = -31.838112 km     theta = 78.091924 deg

        Ring WCR3
G. o. f. (trans) = 1.247327
G. o. f. (size) = 0.043437
deltax = -174.106305 km     deltay = -165.480042 km     theta = 46.455130 deg

        Ring CCR1
G. o. f. (trans) = 0.259344
G. o. f. (size) = 0.116005
deltax = -10.592606 km     deltay = 8.432876 km     theta = 51.476366 deg

        Ring CCR2
G. o. f. (trans) = 0.818923
G. o. f. (size) = 0.002000
deltax = 177.028623 km     deltay = 21.383307 km     theta = 83.112603 deg

        Ring CCR3
G. o. f. (trans) = 0.932353
G. o. f. (size) = 0.039793
deltax = -92.959639 km     deltay = 80.256470 km     theta = 49.194398 deg

        Ring CCR4
G. o. f. (trans) = 1.103971
G. o. f. (size) = 0.000200
deltax = -217.999762 km     deltay = 186.531806 km     theta = 49.448003 deg
```

Distribution List

Applied Physics Laboratory
Johns Hopkins University
John Hopkins Road
Laurel MD 20707

Applied Physics Laboratory
University of Washington
1013 NE 40th St.
Seattle WA 98105

Applied Research Laboratory
Pennsylvania State University
P.O. Box 30
State College PA 16801

Applied Research Laboratory
University of Texas at Austin
P.O. Box 8029
Austin TX 78713-8029

Assistant Secretary of the Navy
Research, Engineering & Systems
Washington DC 20350-2000

Chief of Naval Operations
Washington DC 20350-2000
Attn: OP-71
        OP-987

Chief of Naval Operations
Oceanographer of the Navy
34th and Massachusetts Ave., NW
Washington DC 20392-1800
Attn: OP-096
        OP-96B
        Mr. R. Feden

David W. Taylor Naval Research Center
Bethesda MD 20084-5000
Attn: Commander

Defense Mapping Agency
Systems Center
12100 Sunset Hill Rd #200
Reston VA 22090-3207
Attn: Director
        Code SGWN

Director of Navy Laboratories
Crystal Plaza #5, Rm. 1062
Washington DC 20360

Fleet Antisub Warfare Tng Ctr-Atl
Naval Station
Norfolk VA 23511-6495

Fleet Numerical Oceanography Center
Monterey CA 93943-5005
Attn: Commanding Officer
        Dr. M. Clancy
        Mr. J. Cornelius

Louisiana State University
Dept. of Computer Science
Baton Rouge LA 70803-4020
Attn: Dr. S. S. Iyengar

National Ocean Data Center
1825 Connecticut Ave., NW
Universal Bldg. South, Rm. 406
Washington DC 20235
Attn: G. Withee, Director

Naval Air Development Center
Warminster PA 18974-5000
Attn: Commander

Naval Air Systems Command HQ
Washington DC 20361-0001
Attn: Commander

Naval Civil Engineering Laboratoray
Port Hueneme CA 93043
Attn: Commanding Officer

Naval Coastal Systems Center
Panama City FL 32407-5000
Attn: Commanding Officer

Naval Eastern Oceanography Center
McAdie Building
U117
Naval Air Station
Norfolk VA 23511
Attn: Mr. C. A. Weigand

Naval Facilities Engineering
Command HQ
200 Stovall St.
Alexandria VA 22332-2300
Attn: Commander

Naval Oceanographic Office
Stennis Space Center MS 39529
Attn: Commanding Officer
        Code MTA, W. Austin
        Code M, L. J. Bernard
        Code MT, A. A. Johnson
        Code MTR, J. P. Rigney

Naval Oceanography Command
Stennis Space Center MS 39529
Attn: Commander
        Dr. D. Durham,
        Program Integration Dept.
        Dr. P. F. Moersdorf,
        Space Oceanography Programs

Naval Oceanographic & Atmospheric
Research Laboratory
Stennis Space Center MS 39529-5004
Attn: Code 100
        Code 105
        Code 110
        Code 112, Dr. R. M. Root
        Code 113, Dr. B. B. Adams
        Code 115
        Code 125L (10)
        Code 125P
        Code 200
        Code 222, G. A. Kerr
        Code 252, R. S. Romalewski
        Code 300, Dr. H. C. Eppert, Jr.
        Code 320, Dr. J. W. McCaffrey, Jr.
        Code 321, J. D. Hawkins
                R. J. Holyer
                Dr. D. R. Johnson
                D. A. May
                Dr. J. L. Mitchell
                A. E. Pressman
        Code 322, Dr. T. Bennett, Jr.
                M. R. Carnes
                Dr. J. M. Harding
                Dr. A. C. Warn-Varnas
        Code 323, D. N. Fox
                Dr. G. W. Heburn
                Dr. H. E. Hurlburt
                Dr. J. C. Kindle
                Dr. J. D. Thompson, Jr.
        Code 330, Dr. A. W. Green, Jr.
        Code 400

Naval Oceanographic & Atmospheric
Research Laboratory
Monterey CA 93940
Attn: Dr. P. Tag
        Dr. J. Hovermale

Naval Oceanographic & Atmospheric
Research Laboratory
Liaison Office
Crystal Plaza #5, Rm. 802
Arlington VA 22202-5000
Attn: B. Farquhar

Naval Ocean Systems Center
San Diego CA 92152-5000
Attn: Commander

Naval Postgraduate School
Monterey CA 93943
Attn: Superintendent
        Dr. Chin-Hwa Lee,
        Associate Professor,
        Dept. of Electrical
        & Computer Engineering

Naval Research Laboratory
Washington DC 20375
Attn: Commanding Officer

Naval Sea Systems Command HQ
Washington DC 20362-5101
Attn: Commander

Naval Surface Warfare Center
White Oak
10901 New Hampshire Ave.
Silver Spring MD 20904-5000
Attn: Commander
        Library

Naval Surface Weapons Center
Dahlgren VA 22338-5000
Attn: Commander

Naval Underwater Systems Center
Newport RI 02841-5047
Attn: Commander

Naval Underwater Systems Center Det
New London Laboratory
New London CT 06320
Attn: Officer in Charge

Navy Center for Applied Research
in Artificial Intelligence
Naval Research Laboratory
4555 Overlook Ave., S.W.
Washington DC 20375
Attn: Dr. R. P. Shumaker
        Director

NOAA National Ocean Service
Rockville MD 20852
Attn: Dr. R. E. Cheney,
        N/CG11

Office of Naval Research
800 N. Quincy St.
Arlington VA 22217-5000
Attn: Code 10D/10P, Dr. E. Silva
        Code 112, Dr. E. Hartwig
        Code 12
        Code 10

Office of Naval Research
ONR Branch Office
Box 39
FPO New York 09510-0700
Attn: Commanding Officer

Office of Naval Research
Detachment
Stennis Space Center MS 39529
Attn: E. D. Chaika, Director

Office of Naval Technology
800 N. Quincy St.
Arlington VA 22217-5000
Attn: Code 20, Dr. P. Selwyn
        Code 228, Dr. M. Briscoe
        Code 228, CDR L. Bounds
        Code 234, Dr. C. Votaw

Planning Systems, Inc.
PSI Science Center
115 Christian Lane
Slidell LA 70458
Attn: Dr. R. L. Crout,
        Senior Scientist

REPORT DOCUMENTATION PAGE

1. Agency Use Only *(Leave blank)*.	2. Report Date.	3. Report Type and Dates Covered.
	June 1990	Final

4. Title and Subtitle.

Oceanographic Expert System Validation Using GOAP Mesoscale Products and Gulfcast/DART Validation Test Data

6. Author(s).

Matthew Lybanon

5. Funding Numbers.

Program Element No. 63704N

Project No. 0101

Task No. 1001

Accession No. DN394464

7. Performing Organization Name(s) and Address(es).

Naval Oceanographic and Atmospheric Research Laboratory
Ocean Science Directorate
Remote Sensing Branch
Stennis Space Center, Mississippi 39529-5004

8. Performing Organization Report Number.

NOARL Report 5

9. Sponsoring/Monitoring Agency Name(s) and Address(es).

Space and Naval Warfare Systems Command
Washington, DC 20363-5100

10. Sponsoring/Monitoring Agency Report Number.

11. Supplementary Notes.

12a. Distribution/Availability Statement.

Approved for public release: distribution is unlimited. Naval Oceanographic and Atmospheric Research Laboratory, Stennis Space Center, Mississippi 39529-5004.

12b. Distribution Code.

13. Abstract *(Maximum 200 words)*.

A prototype oceanographic expert system is being developed by the Remote Sensing Branch of the Naval Oceanographic and Atmospheric Research Laboratory (NOARL). System performance for eddy motion was tested using GEOSAT Ocean Applications Program (GOAP) mesoscale products. A second data set was used to validate the Harvard Gulfcast and the NOARL DART (Data Assimilation Research and Transition program) models.

Several types of performance measures were calculated for both warm- and cold-core Gulf Stream eddies. Statistics compiled from the analysis results are presented in both tabular and graphical form. The analysis shows that the expert system performs reasonably well with respect to both eddy motion and eddy size. The expert system's projections are superior to an assumption of no motion out to 14 days. Results with the second (better) data set indicate performance superior to no motion in about two-thirds of the cases. The GOAP results, which used longer sequences, indicate that the cold-core ring rules perform well for periods longer than 2 weeks. The expert system tracks ring sizes to within 10% for periods up to 7-11 weeks.

Discussion of the results identifies factors that interfere with the validation and strongly indicates the need for more data to continue and refine the analysis. A first-order correction to the rule base is proposed, based on the results of this study. That correction should significantly improve the expert system's average eddy motion performance. Changes based upon a more detailed evaluation may also be feasible and could lead to greater improvements.

14. Subject Terms.

GEOSAT, expert system, rule base, Gulf Stream

15. Number of Pages.
32

16. Price Code.

17. Security Classification of Report.	18. Security Classification of This Page.	19. Security Classification of Abstract.	20. Limitation of Abstract.
Unclassified	Unclassified	Unclassified	None